

Published in final edited form as:

Nature. 2012 August 9; 488(7410): 222–225. doi:10.1038/nature11242.

HVEM signalling at mucosal barriers provides host defence against pathogenic bacteria

Jr-Wen Shui¹, Alexandre Lorange¹, Gisen Kim¹, Jose Luis Vela¹, Sonja Zahner¹, Hilde Cheroutre¹, and Mitchell Kronenberg¹

¹Division of Developmental Immunology, La Jolla Institute for Allergy and Immunology, 9420 Athena Circle, La Jolla, California 92037, USA

Abstract

The herpes virus entry mediator (HVEM), a member of the tumour-necrosis factor receptor family, has diverse functions, augmenting or inhibiting the immune response¹. HVEM was recently reported as a colitis risk locus in patients², and in a mouse model of colitis we demonstrated an anti-inflammatory role for HVEM³, but its mechanism of action in the mucosal immune system was unknown. Here we report an important role for epithelial HVEM in innate mucosal defence against pathogenic bacteria. HVEM enhances immune responses by NF- κ B-inducing kinase-dependent Stat3 activation, which promotes the epithelial expression of genes important for immunity. During intestinal *Citrobacter rodentium* infection^{4–6}, a mouse model for enteropathogenic *Escherichia coli* infection, *Hvem*^{-/-} mice showed decreased Stat3 activation, impaired responses in the colon, higher bacterial burdens and increased mortality. We identified the immunoglobulin superfamily molecule CD160 (refs 7 and 8), expressed predominantly by innate-like intraepithelial lymphocytes, as the ligand engaging epithelial HVEM for host protection. Likewise, in pulmonary *Streptococcus pneumoniae* infection⁹, HVEM is also required for host defence. Our results pinpoint HVEM as an important orchestrator of mucosal immunity, integrating signals from innate lymphocytes to induce optimal epithelial Stat3 activation, which indicates that targeting HVEM with agonists could improve host defence.

Because HVEM functions in the colonic mucosa^{2,3,10}, we explored its role in colonic epithelial cells, a cell type whose barrier function is critical for preventing colitis pathogenesis and enhancing mucosal defence¹¹. In addition to leukocytes that carry the CD45 antigen, HVEM is expressed by epithelial cells in the colon and lung, as well as by mouse epithelial cell lines CMT-93 (colon) and LA-4 (lung) (Supplementary Fig. 1). When stimulated *in vitro* by known HVEM ligands, either a fusion protein containing the B- and T-lymphocyte attenuator (BTLA-Ig) or recombinant CD160, CMT-93 cells, colon fragments in culture or primary colonic epithelial cells could be induced to produce innate immune mediators essential for host protection (Fig. 1a and Supplementary Fig. 2). These included genes encoding anti-microbial proteins, such as Reg3 $\beta/3\gamma$, β -defensin 3 and S100A9, proinflammatory cytokines IL-6, IL-1 β and tumour-necrosis factor (TNF), as well as chemokines. As epithelial cells produce these mediators, our data suggest that it was

Correspondence and requests for materials should be addressed to M.K. (mitch@liai.org).

Full Methods and any associated references are available in the online version of the paper at www.nature.com/nature.

Author Contributions J.-W.S., A.L., G.K., J.L.V. and S.Z. designed and performed the experiments. H.C. and M.K. contributed to experimental design. J.-W.S. and M.K. wrote the manuscript.

Reprints and permissions information is available at www.nature.com/reprints. The authors declare no competing financial interests. Readers are welcome to comment on the online version of this article at www.nature.com/nature.

Supplementary Information is linked to the online version of the paper at www.nature.com/nature.

HVEM signalling in epithelium that regulated innate immune responses in the colon fragments. Interestingly, the innate immune mediators that were increased in epithelial cells are also induced by IL-22R signalling, which acts through Stat3 (refs 12 and 13). Although, like other TNF receptors, HVEM signals through TRAF proteins to activate NF- κ B¹⁴, we found that HVEM engagement by its ligands also induced Stat3 phosphorylation in epithelial cells and colon fragment cultures (Fig. 1b and Supplementary Fig. 3). Interestingly, HVEM engagement did not induce immediate Stat3 activation in leukocytes, and although HVEM signalling has been reported to promote NF- κ B-inducing kinase (NIK)-Stat3-dependent Th17 cell differentiation *in vitro*¹⁵, this may require extra and/or more prolonged stimulation. By contrast, the rapid HVEM-mediated Stat3 activation in epithelial cells emphasizes the direct connection of HVEM signals to Stat3 phosphorylation. We further determined that HVEM-induced Stat3 activation was NIK-dependent (Fig. 1c and Supplementary Fig. 4). As Stat3 activity is associated with epithelial responses¹³, our results indicate that NIK, upstream of Stat3, links epithelial HVEM signalling to mucosal innate immunity and host defence.

IL-22 is essential for host defence because it induces epithelial production of cytokines, chemokines and anti-microbial peptides, and promotes epithelial recovery from mucosal injury^{12,16–21}. Although IL-22 signalling also induces epithelial Stat3 activation and gene expression, we found signalling by IL-22R did not require NIK (Fig. 1c). This suggests that the HVEM–Stat3 pathway is independent of the IL-22–Stat3 pathway. Indeed, we found that IL-22 induced Stat3 activation and epithelial gene expression in the absence of HVEM signalling and vice versa (Fig. 1d). However, HVEM and IL-22 signalling exhibited additive effects on Stat3 activation (Fig. 1b) and gene expression (Supplementary Fig. 2). As such, we reasoned that a fully activated Stat3, cooperatively regulated by IL-22R and HVEM, probably is important for intestinal epithelial responses and host defence.

We tested this hypothesis using *C. rodentium* infection, a mouse model for acute attaching/effacing enteropathogenic *E. coli* infection in humans⁴. We found that *Hvem*^{-/-} mice had reduced survival, higher bacterial burdens in colons and faeces and increased colonic epithelial permeability after infection and bacterial dissemination (Fig. 2a–c and Supplementary Fig. 5). The compromised epithelial integrity and responses after infection probably contributed to bacterial translocation and lethality. As a consequence of the poorly controlled bacterial burdens, *Hvem*^{-/-} mice suffered more severe colonic hyperplasia (at day 14) and pathology (at day 14 and 21) after infection (Fig. 2c and Supplementary Fig. 5). Analysis of infected *Hvem*^{-/-}*Rag*^{-/-} mice also showed an impaired production of epithelial mediators and increased pathology compared with *Rag*^{-/-} mice (Supplementary Fig. 6), indicating a role for HVEM expression independent of adaptive immunity. Consistent with a role for epithelial HVEM, using bone-marrow chimaeric mice, we found that HVEM expression by radiation-resistant cells in the recipients was required for host protection (Fig. 2d).

Because HVEM binds to the TNF superfamily member LIGHT, and immunoglobulin (Ig) superfamily members BTLA and CD160 (ref. 1), we performed experiments to identify which is the important ligand(s) for HVEM in the intestine. *Light*^{-/-}, *Btla*^{-/-} and *Light*^{-/-}*Btla*^{-/-} double knockout mice were able to clear bacteria similarly to wild-type mice (Supplementary Fig. 7), suggesting that neither HVEM-LIGHT nor HVEM-BTLA signalling is required for host defence against *C. rodentium*. By contrast, mice injected with an anti-CD160 blocking but non-depleting antibody showed impaired host defence (Fig. 3a and Supplementary Figs 8 and 9), indicating that CD160 is essential. We performed colon fragment cultures, *in vitro* infected with *C. rodentium*, which targets epithelial cells^{5,22}, to explore further the ligand necessary for HVEM engagement. We found *Hvem*^{-/-}, *Il-22r1*^{-/-} or anti-CD160 treated wild-type colons, but not *Light*^{-/-} or *Btla*^{-/-} colons, showed reduced

expression of host defence mediators (Supplementary Fig. 10 and data not shown). CD160 also interacts with some major histocompatibility complex (MHC) class I molecules⁷, but CD160 blockade in *Hvem*^{-/-} colons did not cause an alteration in the innate immune response or survival in infected mice (Supplementary Fig. 10).

To determine the *in vivo* function of HVEM-CD160 signalling further, we analysed the caecum at day 2 after infection, because *C. rodentium* is known to colonize this part of the intestine first⁴. We found *Hvem*^{-/-} and *Il-22r1*^{-/-} mice, as well as anti-CD160 injected mice, had impaired caecal expression of host defence genes (Fig. 3b). Cytokine and chemokine protein production was also reduced in the colons of infected *Hvem*^{-/-} mice (Supplementary Fig. 11). Furthermore, caecal Stat3 activation was significantly reduced in *Hvem*^{-/-} and *Il-22r1*^{-/-} mice, as well as in anti-CD160 injected mice (Fig. 3c and Supplementary Fig. 12). These results indicate that by regulating epithelial Stat3 activation, both the CD160–HVEM and IL-22–IL-22R signalling pathways are essential for epithelial innate function and mucosal host defence. Supporting this, we observed that mice with an epithelial cell-specific IL-22R1 deletion (*Vil-Cre;Il-22r1^{lox/lox}*) were also susceptible to *C. rodentium* infection, similar to *Hvem*^{-/-} mice (Supplementary Fig. 10d).

We determined if the two pathways of Stat3 activation in epithelial cells influence one another. Similar to the action of several other cytokines on their receptors, IL-22 upregulated expression of its own receptor (Fig. 3d), specifically the IL-22R1 subunit, but not the IL-10R2 chain shared with several other cytokines. Interestingly, expression of IL-22R1 was also increased after HVEM engagement in CMT-93 cells and colon fragments. Furthermore, early after bacterial infection, colonic IL-22R1 expression was reduced in *Hvem*^{-/-} and anti-CD160-injected mice (Fig. 3d and Supplementary Fig. 13). These results indicate that HVEM, in addition to activating Stat3 independently of the IL-22 receptor, could cross-regulate IL-22R signalling and sensitize epithelium by promoting IL-22R1 expression. This would render epithelial cells more responsive to bacterial infection. Consistent with this model for the regulation of receptor expression is the fact that the human and mouse *Il22r1* promoters contain both Stat and NF- κ B binding sites^{23,24}, which could be the targets of Stat3 and NF- κ B activated by HVEM²⁵.

Epithelial Reg3 β/γ was shown to be a major target of Stat3 signalling during mucosal inflammation¹³ and was important for host protection against *C. rodentium*¹². As HVEM induced epithelial Reg3 expression, and there was a dramatic decrease in Stat3 activation and Reg3 β/γ expression in *Hvem*^{-/-} colons during infection, it is likely that colonic Reg3 expression, mediated by HVEM–Stat3, contributed to host protection. Indeed, recombinant Reg3 γ protein administered to *Hvem*^{-/-} mice protected them from lethal infection and significantly reduced bacterial burdens in faeces (Supplementary Fig. 14). These results indicate that the HVEM–Stat3–Reg3 pathway in the epithelium provides host protection during intestinal infection.

Both BTLA and CD160 could trigger HVEM signalling and induce epithelial Stat3 activation and production of host defence mediators *in vitro*; however, it is still uncertain why only CD160 was essential for host protection *in vivo*. When expression levels of the three HVEM ligands in colonic intraepithelial lymphocytes (IELs), lamina propria lymphocytes (LPLs) and splenocytes were compared, we found that CD160 was almost exclusively expressed by IELs (Fig. 3e). There were very low messenger RNA (mRNA) levels of BTLA and LIGHT in IELs, providing an explanation why these were not functional ligands for HVEM after *C. rodentium* infection. A more detailed analysis of the IEL and LPL compartments during bacterial infection revealed that the CD8 α^+ CD8 β^- CD160⁺ IEL population was rapidly increased at the early stage of infection (Fig. 3f and Supplementary Fig. 15). These CD160⁺ IELs with the CD8 $\alpha\alpha$ homodimer

expression consisted of both T-cell receptor (TCR) $\alpha\beta$ and TCR $\gamma\delta$ T subsets, but the TCR $\gamma\delta$ IELs became more prevalent after infection (Supplementary Fig. 15). Furthermore, CD160 was also expressed by TCR-negative IELs in *Rag*^{-/-} mice, which presumably provide a physiological ligand for epithelial HVEM in the absence of adaptive immunity (Supplementary Fig. 16). Together, these results provide evidence that CD160 expressed by several IEL subsets, particularly the innate-like CD8 $\alpha\alpha$ -expressing cells, represents the only ligand available for engaging epithelial HVEM in the intestine. Furthermore, the increase in CD8 $\alpha\alpha$ ⁺CD160⁺ IELs during early infection is consistent with the hypothesis that the HVEM-CD160 interaction at the mucosal surface enhances signalling in epithelial cells and promotes their innate response to acute bacterial infection. It remains possible, however, that the contribution of the HVEM-CD160 signal is regulated in other ways, for example by the removal of an inhibitor in one of the interacting cell types.

To determine if HVEM mediates epithelial host defence at other mucosal sites, we examined the immune response of *Hvem*^{-/-} mice after lung infection with *S. pneumoniae*, a Gram-positive extracellular bacteria that is the most common cause of community-acquired pneumonia^{26,27}. We found *Hvem*^{-/-} mice were highly susceptible to *S. pneumoniae*, with an impaired early host response leading to reduced bacterial elimination in the lung (Fig. 4a). Similar to the role of HVEM in colonic epithelium, the reduced innate immune response in the lung epithelium early after infection probably contributed to the impaired host defence in *Hvem*^{-/-} mice (Fig. 4b and Supplementary Fig. 17). Stat3 signalling in the alveolar epithelium is essential for host defence to limit bacteria-induced pneumonia^{26,28,29}. Similar to the intestinal mucosae, HVEM stimulation induced Stat3 phosphorylation in the lung and Stat3 activation was significantly decreased in the lung of *Hvem*^{-/-} mice at the early stage of *S. pneumoniae* infection (Fig. 4c and Supplementary Fig. 18). This indicates HVEM-Stat3 signalling regulates epithelial responses in the lung and mediates host defence against pulmonary bacteria. LA-4 cells, a lung epithelial cell line, also express HVEM (Supplementary Fig. 1c). When these cells were stimulated *in vitro* to trigger HVEM signalling, the expression of several epithelial host defence genes was significantly induced (Fig. 4d), indicating HVEM directly regulates lung epithelial immune function.

HVEM is an unusual TNF receptor family member in binding TNF as well as Ig superfamily molecules, and in serving as a ligand for inhibitory receptors such as BTLA, as well as being a signalling receptor itself. We have revealed that HVEM, acting as a signalling receptor on epithelial cells, leads to NIK-dependent Stat3 activation, thereby inducing the expression of genes important for host defence in the intestine and lung. Furthermore, we demonstrated that in the intestine CD160 on CD8 $\alpha\alpha$ ⁺ IELs is the functional ligand for triggering epithelial HVEM for host protection. Human CD160 expression on IELs and epithelial HVEM expression have been described^{8,30}, but it is not known if this interaction has a role in humans. HVEM signalling also promotes epithelial IL-22R1 expression, which renders epithelial cells more responsive to IL-22, a major innate cytokine critical for host defence. Our results therefore show that HVEM is a crucial regulator of epithelial innate responses, in part by mediating lymphocyte-epithelial communication, and by cooperating with IL-22R signalling to induce optimal epithelial Stat3 activation for host defence.

METHODS

Animal manipulations

C57BL/6 and *Rag*^{-/-} mice were purchased from the Jackson Laboratory and bred in-house for all experiments. *Hvem*^{-/-}, *Hvem*^{-/-} *Rag*^{-/-}, *Btla*^{-/-}, *Light*^{-/-} and *Light*^{-/-} *Btla*^{-/-} mice have been bred and described previously³. *Il-22r1* flox (knockout first) mice on the C57BL/6 background were obtained from The European Conditional Mouse Mutagenesis Program (EUCOMM) and were bred to Vil-Cre mice for conditional IL-22R1 deletion in epithelium

(*Vil-Cre;II-22r1^{flox/flox}*). All gene-deficient mice were backcrossed for at least eight generations onto the C57BL/6 background. Mice were used at 8–12 weeks of age. Whenever possible, control and gene knockout mice were housed in the same cage to minimize the effect of housing conditions on experimental variation. For tissue or cell analyses, tissues were collected and used for histological analysis, intraepithelial and lamina propria cell preparation, total protein or RNA isolation. For the rescue experiment, Reg3 γ -Ig fusion protein (150 μ g per mouse per time point, provided by Genentech) was injected intraperitoneally into mice on days 1, 3, 5, 7 and 9 after infection as previously described¹². For the blocking experiment, anti-mouse CD160 or IgG_{2a} isotype control antibodies (100 μ g per mouse per time point) was injected intraperitoneally into mice on days -1, 1, 3, 5, and 7 after infection.

Bacterial infection

A wild-type *C. rodentium* strain DBS100 rendered resistant to chloramphenicol and a clinical strain of *S. pneumoniae* (serotype 3, URF918) were obtained and used in all infection studies^{6,9}. For *C. rodentium*, bacteria were grown overnight in Luria-Bertani broth with shaking at 37 °C for 15–16 h. For *S. pneumoniae*, bacteria were grown to mid-log phase for 6–7 h from a frozen stock in Todd-Hewitt broth. Bacterial cultures were adjusted with PBS for proper concentration and individual titres were determined after each experiment by serial dilution. Mice were infected with 0.5×10^9 to 3.5×10^9 c.f.u. (*C. rodentium*, by oral gavage) or 1×10^6 to 5×10^6 c.f.u. (*S. pneumoniae*, by retropharyngeal instillation), and were killed at the indicated time points after infection. For c.f.u. assays, spleen, lung, liver, mesenteric lymph node, faecal pellets or colon were weighed, homogenized, serially diluted and plated in chloramphenicol-containing MacConkey (for *C. rodentium*) or Columbia sheep blood (for *S. pneumoniae*) agar plates.

Epithelial cell lines and reagents

Mouse colonic (CMT-93, number CCL-223) and lung (LA-4, number CCL-196) epithelial cell lines were obtained from American Type Culture Collection and were maintained in DMEM (CMT-93) or F12-K (LA-4) medium (Invitrogen), supplemented with 10–15% FBS, penicillin and streptomycin. Cells were cultured in six-well (for protein analysis) or 12-well (for quantitative real-time PCR analysis) plates and were serum starved for 24 h before *in vitro* stimulation. Recombinant mouse IL-22, CD160, LIGHT, BTLA Fc chimaeric fusion protein (BTLA-Ig) and mouse IgG_{2a} Fc (control-Ig) were purchased from R&D Systems and used for *in vitro* stimulation experiments at the indicated concentrations. Anti-mouse CD160 (CNX46-3) and IgG_{2a} isotype control antibodies (both from eBioscience) were used for *in vivo* blocking experiments. A short interfering RNA Kit for NIK knockdown was obtained from Qiagen (GS53859). The short interfering RNA sequences for NIK (*Map3k14*) knockdown were *Map3k14_1* (CTGGGT CAGCTCATAAAGCAA), *Map3k14_2* (CCCTTGAAAGGAGAATATAA), *Map3k14_3* (TAGCATTAAAGTTCCTACTGTGAA) and *Map3k14_4* (CAGGAAGA TGAGTCTCCACTA).

Ex vivo infection of colons

Distal colons were freshly isolated from mice, cleaned and cut into several small pieces (~3 mm). Colon fragments were then transferred to six-well plate containing 3 ml of DMEM supplemented with 10% FBS and antibiotics. Live *C. rodentium* were added to each well (10^7 – 10^8 c.f.u. ml⁻¹) and incubated for 20–24 h. After incubation, *ex vivo* infected colons were collected, briefly washed, and total RNA was extracted using an RNeasy Kit (Qiagen).

Preparation of colonic epithelial cells

Primary epithelial cells were isolated as described previously³¹. Briefly, colons were cut open longitudinally, and epithelial cells were separated by shaking the small colon pieces in HBSS containing 5% FBS, 5 mM EDTA and 1 mM DTT for 15 min. The remaining tissue was discarded and epithelial cells in the supernatant were spun down at 150g for 5 min. The cell pellets were re-suspended in 40% Percoll solution and spun down again. The epithelial cells at the top layer were collected. These cells were stained with epithelial cell specific markers anti-cytokeratin-18 (C-04, Abcam) and anti-EpCAM (G8.8, eBioscience) to estimate purity (>95%).

Preparation of IELs and LPLs

Small and large intestines were collected from mice. Peyer's patches were carefully removed and tissues were cut open longitudinally, briefly washed, and cut into 1.5 cm pieces. The tissue pieces were incubated in 30 ml of HBSS (5% FBS, 10 mM HEPES and 1 mM DTT) in a shaker at 250 r.p.m., 37 °C, for 30 min. After incubation, the cell suspension was intensively vortexed and filtered through a metal mesh. The tissue debris was saved for LPL preparation and the flow-through cell suspension, which constitutes the epithelial cell content and IELs, was spun down at 230g for 5 min. The cell pellets were then re-suspended in 40% Percoll solution and overlaid above a 70% Percoll solution. The gradient was spun at 800g for 25 min and IELs at the interface after spin were collected. For LPL preparation, the tissue debris was incubated in 20 ml of HBSS (5% FBS, 5 mM EDTA) in a shaker at 250 r.p.m., 37 °C, for 20 min to further remove epithelial cells. After that, tissues were further cut into 1 mm pieces, placed in 20 ml pre-warmed digestion solution containing 1.5 mg ml⁻¹ collagenase type VIII (Sigma) and incubated at 37 °C for 20 min with rotation. After incubation, digested tissues were filtered through a metal mesh. The flow-through cell suspension was spun down and the re-suspended cells were further purified by Percoll gradient centrifugation. LPLs were collected at the interface, washed once and re-suspended in complete RPMI-1640 medium. The cells were used immediately for cell counting and staining.

Generation of bone-marrow chimaeras

Recipient mice (wild-type or *Hvem*^{-/-} in C57BL/6, Ly5.2 background) were lethally irradiated with 12 Gy that were applied in two doses of 6 Gy separated by a 3 h interval, as previously described³. After irradiation, hosts were transplanted with 7×10^6 total bone-marrow cells isolated from wild-type congenic C57BL/6 or *Hvem*^{-/-} mice on the Ly5.1 background to generate three groups ($n = 6$ in each group) of chimaeric animals as follows: WT(Ly5.1) bone-marrow to WT(Ly5.2) host, WT(Ly5.1) bone-marrow to *Hvem*^{-/-}(Ly5.2) host, and *Hvem*^{-/-}(Ly5.1) bone-marrow to WT(Ly5.2) host. After transplant, mice were maintained with antibiotic treatment for the first week and an additional 11 weeks without antibiotic treatment. Mice were checked at 8 weeks after transplant for reconstitution by surface staining of peripheral blood cells for Ly5.1⁺ expression (>95% in lymphocytes in all cases).

FITC-dextran permeability assay

In vivo permeability assays to assess intestinal barrier function were performed using FITC-labelled dextran (Sigma) as described previously³². Briefly, mice were infected with *C. rodentium*. At day 7 or day 12 after infection, mice were gavaged with FITC-dextran (60 mg per 100 g body weight) and serum was collected retro-orbitally 7–8 h later. Blood cells in serum samples were removed and the fluorescence intensity of FITC-dextran was measured. FITC-dextran concentrations were determined from standard curves generated by serial dilution.

Western blotting and ELISA

Cell lines or colon fragments, were *in vitro* stimulated as indicated; to reduce background from the cell lines they were serum starved for 24 h. Cells or tissues were directly lysed in RIPA buffer supplemented with a protease and phosphatase inhibitor cocktail (Thermo Scientific). Protein lysates were analysed by SDS–polyacrylamide gel electrophoresis (Bio-Rad) and membranes were blotted with anti-Stat3 and anti-phosphorylated Stat3 antibodies (Cell Signaling). For ELISA, supernatants from colon fragment cultures were collected and analysed by R&D Quantikine ELISA Kits according to the manufacturer's instructions.

Flow cytometry and antibodies

Flow cytometry analysis was on an LSRII instrument (BD Biosciences) and we analysed data using Flowjo software (Tree Star). The following mouse antibodies were purchased from BD PharMingen or eBiosciences: CD45 (30-F11), TCR β (H57-597), TCR $\gamma\delta$ (eBio-GL3), CD8 α (53-6.7), CD8 β (eBioH35-17.2), BTLA (6F7), pStat3 (clone 4/P-STAT3), IL-1 β (NJTEN3), TNF (MP6-XT22) and CD160 (CNX46-3). Anti-mouse HVEM (HMHV-1B18) antibody was from Biolegend. Anti-mouse IL-22R1 (clone 496514), anti-CCL20 (clone 114906) and anti-CXCL1-Biotin antibodies were purchased from R&D Systems.

Histology analysis

Histopathological analysis of colon samples was performed on formalin-fixed tissue after haematoxylin and eosin staining. Five different histological categories (oedema, inflammation severity, internal bleeding in the gut tissue, crypt damage, percentage of involvement) were scored with a maximum score of 2 or 3 in each category. Maximal total score is 14 for severity of colitis.

Real-time PCR analysis

Total RNA was extracted from infected tissues using an RNeasy Kit (Qiagen), according to the manufacturer's instructions. cDNA synthesis was performed with an iScript cDNA Synthesis Kit (Bio-rad). Quantitative real-time PCR reactions were performed with the SYBR Green I Master Kit and LightCycler 480 system (Roche). All mRNA levels shown in figures were normalized to the housekeeping gene *L32* and a multiplier of 10^4 was indicated when compared with *L32* levels. The primer sets used were described previously^{12,33}.

Statistics

All data were analysed using GraphPad Prism 5 software and were shown as mean and the standard error of the mean (s.e.m.). Two-tailed unpaired Student's *t*-tests were used to analyse the results. Differences indicated and considered significant when $P < 0.05$.

Supplementary Material

Refer to Web version on PubMed Central for supplementary material.

Acknowledgments

This work was supported by grants from the National Institutes of Health (RO1-AI061516 to M.K.; PO1 DK46763 to M.K.; F32-DK082249 to J.-W.S.; F32-AI083029 to J.L.V.), La Jolla Institute for Allergy and Immunology and the Center for Infectious Disease (LIAI-JAN-2011-CID to J.-W.S.). We thank W. Quyang for providing Reg3 γ -Ig fusion protein, and O. Turovskaya for performing histology staining and pathological scoring. We also thank C. Benedict for providing *NIK^{aly/aly}* mice, K. Pfeffer for providing *Hvem^{-/-}* and *Light^{-/-}* mice and K. Murphy for *Btla^{-/-}* mice. This is manuscript number 1347 from the La Jolla Institute for Allergy and Immunology.

References

1. Murphy TL, et al. Slow down and survive: enigmatic immunoregulation by BTLA and HVEM. *Annu Rev Immunol.* 2010; 28:389–411. [PubMed: 20307212]
2. Anderson CA, et al. Meta-analysis identifies 29 additional ulcerative colitis risk loci, increasing the number of confirmed associations to 47. *Nature Genet.* 2011; 43:246–252. [PubMed: 21297633]
3. Steinberg MW, et al. A crucial role for HVEM and BTLA in preventing intestinal inflammation. *J Exp Med.* 2008; 205:1463–1476. [PubMed: 18519647]
4. Mundy R, et al. *Citrobacter rodentium* of mice and man. *Cell Microbiol.* 2005; 7:1697–1706. [PubMed: 16309456]
5. Ma C, et al. *Citrobacter rodentium* infection causes both mitochondrial dysfunction and intestinal epithelial barrier disruption *in vivo*: role of mitochondrial associated protein (Map). *Cell Microbiol.* 2006; 8:1669–1686. [PubMed: 16759225]
6. LeBlanc PM, et al. Caspase-12 modulates NOD signaling and regulates antimicrobial peptide production and mucosal immunity. *Cell Host Microbe.* 2008; 3:146–157. [PubMed: 18329614]
7. Maeda M, et al. Murine CD160, Ig-like receptor on NK cells and NKT cells, recognizes classical and nonclassical MHC class I and regulates NK cell activation. *J Immunol.* 2005; 175:4426–4432. [PubMed: 16177084]
8. Anumanthan A, et al. Cloning of BY55, a novel Ig superfamily member expressed on NK cells, CTL, and intestinal intraepithelial lymphocytes. *J Immunol.* 1998; 161:2780–2790. [PubMed: 9743336]
9. Nakamatsu M, et al. Role of interferon-gamma in V α 14⁺ natural killer T cell-mediated host defense against *Streptococcus pneumoniae* infection in murine lungs. *Microbes Infect.* 2007; 9:364–374. [PubMed: 17314060]
10. Schaer C, et al. HVEM signalling promotes colitis. *PLoS ONE.* 2011; 6:e18495. [PubMed: 21533159]
11. Artis D, et al. Epithelial-cell recognition of commensal bacteria and maintenance of immune homeostasis in the gut. *Nature Rev Immunol.* 2008; 8:411–420. [PubMed: 18469830]
12. Zheng Y, et al. Interleukin-22 mediates early host defense against attaching and effacing bacterial pathogens. *Nature Med.* 2008; 14:282–289. [PubMed: 18264109]
13. Pickert G, et al. STAT3 links IL-22 signaling in intestinal epithelial cells to mucosal wound healing. *J Exp Med.* 2009; 206:1465–1472. [PubMed: 19564350]
14. Marsters SA, et al. Herpesvirus entry mediator, a member of the tumor necrosis factor receptor (TNFR) family, interacts with members of the TNFR-associated factor family and activates the transcription factors NF- κ B and AP-1. *J Biol Chem.* 1997; 272:14029–14032. [PubMed: 9162022]
15. Jin W, et al. Regulation of Th17 cell differentiation and EAE induction by MAP3K NIK. *Blood.* 2009; 113:6603–6610. [PubMed: 19411637]
16. Liang SC, et al. Interleukin (IL)-22 and IL-17 are coexpressed by Th17 cells and cooperatively enhance expression of antimicrobial peptides. *J Exp Med.* 2006; 203:2271–2279. [PubMed: 16982811]
17. Sugimoto K, et al. IL-22 ameliorates intestinal inflammation in a mouse model of ulcerative colitis. *J Clin Invest.* 2008; 118:534–544. [PubMed: 18172556]
18. Wolk K, et al. Biology of interleukin-22. *Semin Immunopathol.* 2010; 32:17–31. [PubMed: 20127093]
19. Zenewicz LA, et al. Innate and adaptive interleukin-22 protects mice from inflammatory bowel disease. *Immunity.* 2008; 29:947–957. [PubMed: 19100701]
20. Wolk K, et al. IL-22 increases the innate immunity of tissues. *Immunity.* 2004; 21:241–254. [PubMed: 15308104]
21. Brand S, et al. IL-22 is increased in active Crohn's disease and promotes proinflammatory gene expression and intestinal epithelial cell migration. *Am J Physiol Gastrointest Liver Physiol.* 2006; 290:G827–G838. [PubMed: 16537974]
22. Torchinsky MB, et al. Innate immune recognition of infected apoptotic cells directs T(H)17 cell differentiation. *Nature.* 2009; 458:78–82. [PubMed: 19262671]

23. Tachiiri A, et al. Genomic structure and inducible expression of the IL-22 receptor alpha chain in mice. *Genes Immun.* 2003; 4:153–159. [PubMed: 12618864]
24. Gelebart P, et al. Interleukin 22 signaling promotes cell growth in mantle cell lymphoma. *Transl Oncol.* 2011; 4:9–19. [PubMed: 21286373]
25. Cheung TC, et al. Unconventional ligand activation of herpesvirus entry mediator signals cell survival. *Proc Natl Acad Sci USA.* 2009; 106:6244–6249. [PubMed: 19332782]
26. Quinton LJ, et al. Functions and regulation of NF- κ B RelA during pneumococcal pneumonia. *J Immunol.* 2007; 178:1896–1903. [PubMed: 17237440]
27. Mizgerd JP, et al. Animal models of human pneumonia. *Am J Physiol Lung Cell Mol Physiol.* 2008; 294:L387–L398. [PubMed: 18162603]
28. Quinton LJ, et al. NF- κ B and STAT3 signaling hubs for lung innate immunity. *Cell Tissue Res.* 2011; 343:153–165. [PubMed: 20872151]
29. Quinton LJ, et al. Alveolar epithelial STAT3, IL-6 family cytokines, and host defense during *Escherichia coli* pneumonia. *Am J Respir Cell Mol Biol.* 2008; 38:699–706. [PubMed: 18192501]
30. Rooney IA, et al. The lymphotoxin-beta receptor is necessary and sufficient for LIGHT-mediated apoptosis of tumor cells. *J Biol Chem.* 2000; 275:14307–14315. [PubMed: 10799510]
31. Zaki MH, et al. The NLRP3 inflammasome protects against loss of epithelial integrity and mortality during experimental colitis. *Immunity.* 2010; 32:379–391. [PubMed: 20303296]
32. Lebeis SL, et al. Interleukin-1 receptor signaling protects mice from lethal intestinal damage caused by the attaching and effacing pathogen. *Citrobacter rodentium Infect Immun.* 2009; 77:604–614.
33. Ishigame H, et al. Differential roles of interleukin-17A and -17F in host defense against mucosal bacterial infection and allergic responses. *Immunity.* 2009; 30:108–119. [PubMed: 19144317]
34. Hofmann J, et al. NIK signaling in dendritic cells but not in T cells is required for the development of effector T cells and cell-mediated immune responses. *J Exp Med.* 2011; 208:1917–1929. [PubMed: 21807870]
35. Shinkura R, et al. Alymphoplasia is caused by a point mutation in the mouse gene encoding NF- κ B-inducing kinase. *Nature Genet.* 1999; 22:74–77. [PubMed: 10319865]

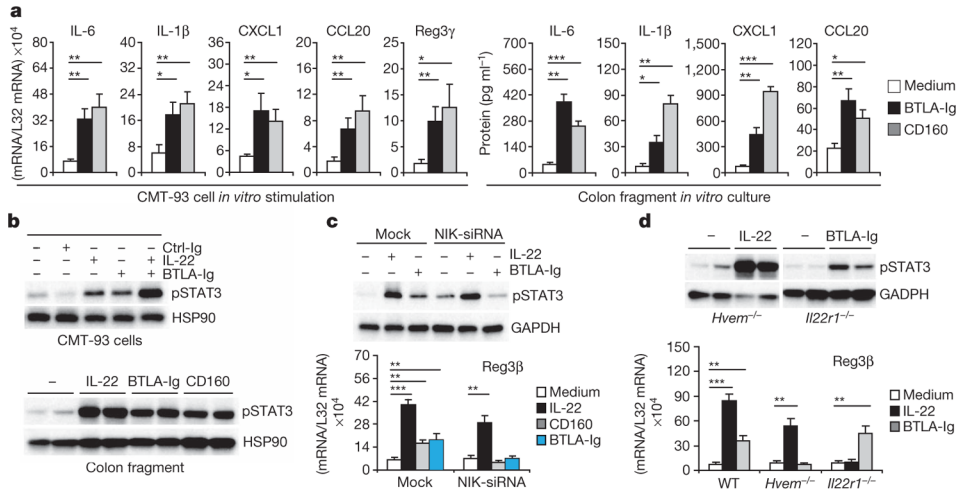


Figure 1. HVEM signalling regulates epithelial immune function by inducing NIK-dependent Stat3 activation

a, HVEM signalling triggered by soluble BTLA-Ig or CD160 induced innate responses in CMT-93 epithelial cells analysed by real-time PCR (left), or in colon fragments analysed by enzyme-linked immunosorbent assay (ELISA) (right). **b**, HVEM signalling induced Stat3 phosphorylation in CMT-93 cells and colon fragments (each lane represents one mouse), determined by western blot. **c**, NIK dependence of HVEM-induced epithelial Stat3 activation and gene expression analysed by NIK short interfering RNA knockdown. **d**, HVEM regulates epithelial Stat3 activation and gene expression independent of IL-22R signalling. Error bars (s.e.m.) are indicated. * $P < 0.05$, ** $P < 0.01$, *** $P < 0.001$ (two-tailed unpaired t -tests). Results were representative of at least two independent experiments.

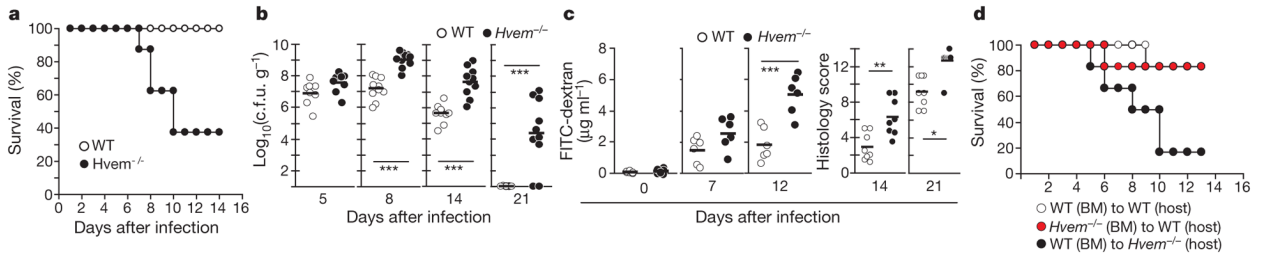


Figure 2. HVEM is required for host defence against intestinal *C. rodentium* infection
 Groups of mice ($n = 6-12$) were infected with *C. rodentium* by oral gavage. **a**, Survival curves for wild-type and *Hvem*^{-/-} mice after infection. **b**, Bacterial burdens in colons after infection. **c**, Epithelial barrier permeability (left), determined by injection of fluorescein isothiocyanate (FITC)-dextran and measurement of fluorescence in the blood, and severe colonic pathology in *Hvem*^{-/-} mice (right). **d**, HVEM expression by non-bone-marrow-derived cells is required for host protection ($n = 6$ in each group of chimaeras). * $P < 0.05$, ** $P < 0.01$, *** $P < 0.001$ (two-tailed unpaired t -tests). Results were representative of at least two independent experiments.

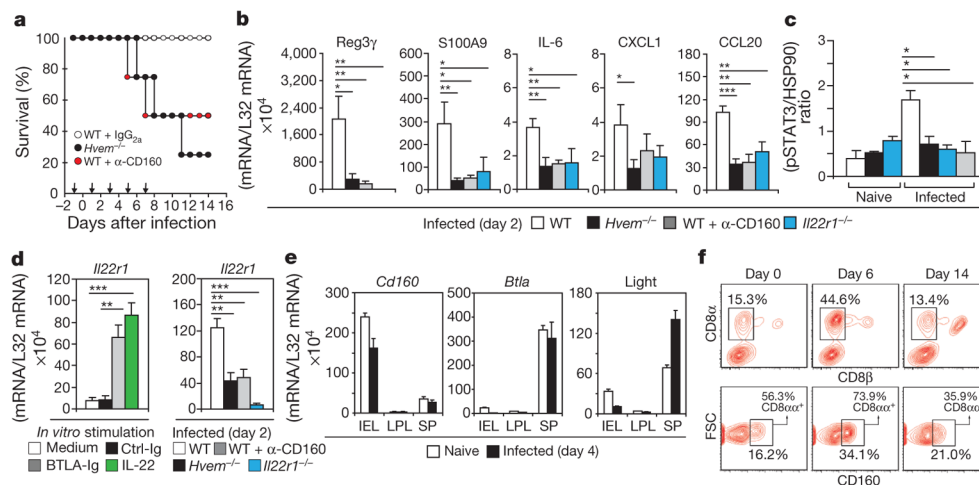


Figure 3. CD160 on IELs provides a ligand for HVEM

a, Survival curves of wild-type (WT), *Hvem*^{-/-} and anti-CD160-injected mice ($n = 4$) after *C. rodentium* infection. Arrows indicate the times of control IgG or anti-CD160 injection. **b**, **c**, Analysis of gene expression (by real-time PCR) and Stat3 phosphorylation (by western blot) in caecal tissues collected from indicated mice at day 2 after infection. **d**, Analysis of *Il22r1* mRNA in stimulated or infected colon fragments. **e**, Analysis of *Cd160*, *Btla* and *Light* mRNA in colonic IELs, LPLs and splenocytes, isolated from naive or infected mice. **f**, Flow cytometry analysis of colonic CD45⁺IELs, isolated from naive or infected mice. * $P < 0.05$, ** $P < 0.01$, *** $P < 0.001$ (two-tailed unpaired t -tests). Results were representative of two independent experiments.

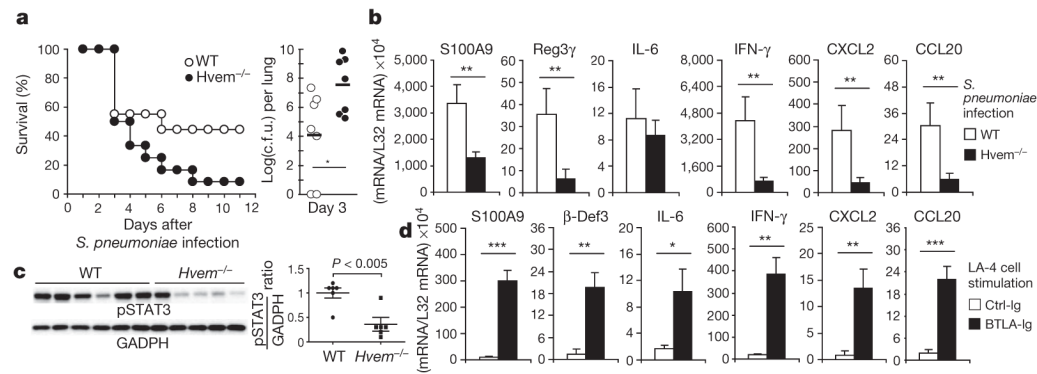


Figure 4. HVEM is required for lung epithelial immunity and host defence against *S. pneumoniae*

Groups of mice ($n = 9-12$) were retropharyngeally infected with *S. pneumoniae* and analysed at the indicated time points. **a**, Survival curves of mice and *S. pneumoniae* c.f.u. in the lung at day 3 after infection. **b**, mRNA expression by real-time PCR in the lung at day 3 after infection. **c**, Analysis of Stat3 phosphorylation in the lung of *S. pneumoniae*-infected mice (each lane represents an individual mouse) at day 2 after infection. **d**, mRNA analysis by real-time PCR in LA-4 lung epithelial cells, stimulated with control-Ig or BTLA-Ig. * $P < 0.05$, ** $P < 0.01$, *** $P < 0.001$ (two-tailed unpaired *t*-tests). Results were representative of two independent experiments.